Published by :
http://www.ijert.org

International Journal of Engineering Research & Technology (IJERT)
ISSN: 2278-0181
Vol. 9 Issue 01, January-2020

Electronic Structure Investigations of 4-Aminophthal Hydrazide

Dr. K. Samuvel, Mr. T.Ravi
Assistant Professor,
Department of Physics,
Dhanalakshmi Srinivasan College of Arts and Science for Women
(Autonomous), Perambalur.

I.Abstract:- **Combined experimental and theoretical studies were conducted on the molecular structure and vibrational spectra of 4-Amino Phthal hydrazide (APH). The FT-IR and FT-Raman spectra of APH were recorded in the hard phase. The molecular geometry and vibrational frequencies of APH in the ground state have been calculated by using the ab initio HF (Hartree-Fock) and density functional methods (B3LYP) invoking 6-311+G(d,p) basis set. The optimized geometric bond lengths and bond angles obtained by the HF method show the best agreement with the experimental values. Evaluation of the experimental fundamental vibrational frequencies of APH with designed results by HF and density functional methods indicate that B3LYP is superior to the scaled Hartree-Fock move towards molecular vibrational problems. The difference between the observed and scaled wavenumber values of most of the fundamentals is very small. A detailed interpretation of the FT-IR and FT- Raman, NMR spectra of APH was also reported. UV–vis spectrum of the compound was recorded and the electronic property, such as HOMO and LUMO energies, were performed by time-dependent density functional theory (TD-DFT) approach. ultimately the results of the calculation were functional to simulated infrared and Raman spectra of the title compound which show good agreement with observed spectra. And the temperature dependence of the thermodynamic properties of constant pressure (Cp), entropy (S) and enthalpy change (ΔH0→T) for APH were also determined.**

Keywords: FTIR, FT-Raman, HOMO- LUMO, NMR, UV, APH

II. INTRODUCTION

Hydrazides and hydrazones, the acylated derivatives [1] of hydrazine besides being useful for many biological properties, hydrazides are important starting material for a wide range of derivatives utilizable in pharmaceutical products and as surfactants. The hydrazones derivatives are used as fungicides, and in the treatment of diseases such as tuberculosis, leprosy, and mental disorders. Biological assessment of fatty hydrazide and the derivatives has been the focus of earlier investigative studies [2,3]. The fatty hydrazides are further derivatives to obtain new antibacterial and antifungal agents. Acylhydrazones, as an example of Schiff bases, and their metal complexes have widely studied due to their versatile applications in the fields of analytical and medicinal chemistry and biotechnology [4-6]. p -Hydroxy benzohydrazide moiety and its analogs seemed to be suitable parent compounds upon which a variety of biological activities were reported such as antitumor, antianginal, antitubercular, antihypertensive and antibacterial [7]. Hydrazides have recently become attractive to theoreticians as well as experimentalists due to the biological significance, particularly in medicinal and enzyme chemistry. A lot of substituted hydrazides are employed in the treatment of psychotic and psychoneurotic conditions. Carboxylic acid hydrazides are known to exhibit strong antibacterial activities that are enhanced by complexation with metal ions. The vibrational spectral studies of hydrazone was analyzed by Durig et al. [8]. The FTIR and FT-Raman spectra of 4-Amino phthalohydrazide (APH), and carried out normal coordinate calculations using the classical method developed by Wilson to support the vibrational analysis [9]. To our knowledge, the literature survey also reveals that to the best of our knowledge no theoretical calculations or detailed vibrational infrared and Raman analysis have been performed on APH molecule so far. A systematic study on the vibrational spectra and structure will aid in understanding the vibrational modes of this title molecule. So, in this work, the vibrational wavenumbers, geometrical parameters, modes of vibrations, minimum energy, 1H, and 13C NMR chemical shifts are calculated with GIAO approach by applying B3LYP method and electrostatic potential also provide information about electronic effects of APH molecule was investigated by using ab initio HF and B3LYP calculations with 6-311+G(d,p) basis set. Specific scale factors were also used and employed in the predicted frequencies. The electronic dipole moment (μ) and the first hyperpolarizability (β) value of the investigate molecule computed show that the APH molecule might have microscopic nonlinear optical (NLO) behavior with non-zero values. The UV spectroscopic studies along with frontier molecular orbital (FMO's) and their energy gaps were analysis. The temperature dependence of the thermodynamic functions and their correlations were performed.

III. EXPERIMENTAL TECHNIQUES

SYNTHESIS PROCEDURE OF 4-AMINOPHTHALHYDRAZIDE

This was performed by adding hydrazine hydrate 10 grams in 20ml water to a suspension of 4-nitrophthalimide (38.4g') in 250ml water and refluxing for one hour. This solution was acidified with acetic acid and cooled and the pale yellow crystalline product was collected with suction. Purification was accomplished with

International Journal of Engineering Research & Technology (IJERT)
ISSN: 2278-0181
Vol. 9 Issue 01, January-2020

a solution in 3 liters boiling 50% acetic acid, rapid filtration, followed by cooling and collection of pale yellow product. The melting point of 4-aminophthalhydrazide 299-300oC. The calculated (found) % for C8H7N3O2: C, 54.24 (53.24); H, 3.98(3.95); N, 23.72 (22.71) and O, 18.06 (17.04). The room temperature Fourier transform infrared (FTIR) spectrum of the title molecule was recorded in the range of 4000-400 cm-1 at a resolution of ± cm-1 using a BRUKER IFS 66V FTIR spectrophotometer equipped with a cooled MCT detector. Boxcar apodization was used for the 250 averaged interferograms collected for both the samples and the background.

The FT-Raman spectrum was recorded on a computer interfaced BRUKER IFS model interferometer, equipped with FRA 106 FT-Raman accessory in the 3500-50 cm-1 Stokes region, using the 1064 nm line of Nd: YAG laser for excitation operating at 200mW power. The reported wave numbers are supposed to be accurate within ±1 cm-1. The UV-visible absorption spectra of APH are examined in the range 200-600 nm using SHIMADZU UV-1650 PC, UV-VIS recording spectrometer. The UV pattern is taken from 10-5 molar solution of APH, solved in ethanol.

COMPUTATIONAL DETAILS

Density functional theory calculations were carried out for APH, Hartree-Fock (HF) and DFT calculations using the GAUSSIAN 09W program package [10]. Initial geometry generated from the standard geometrical parameters was minimized without any constraint on the potential energy surface at the Hartree-Fock level adopting the standard 6-311+G (d,p) basis set. This geometry was then re-optimized again at DFT level employing the B3LYP keyword, which invokes Becke's three-parameter hybrid method [11] using the correlation function of Lee et al.[12], implemented with the same basis set for a better description of the bonding properties of the amino group. All the parameters were authorized to relax and all the calculations converge to an optimized geometry which corresponds to a true minimum, as exposed by the be short of imaginary values in the wavenumber calculations. The multiple scaling of the force constants were performed according to SQM procedure [13] using selective scaling in the natural internal coordinate representation [14]. Transformation of force field, the subsequent normal coordinate analysis including the least square refinement of the scale factors and calculation of the total energy distribution (TED) was done on a PC with the MOLVIB program (version V7.0-G77) written by Sundius [15,16]. The methodical assessment of the results from DFT theory with the results of the experiment has shown that the method using B3LYP well-designed is the most hopeful in providing correct vibrational wavenumbers.

The calculated geometrical parameters were compared with the X-ray diffraction result [17]. Normal coordinate analyses were carried out for the title compound to provide a complete assignment of fundamental frequencies. For this purpose, the full set of 77 standard internal coordinates (containing 23 redundancies) for APH was defined as given in Table 1. From these, a non-redundant set of local symmetry coordinates were constructed by suitable linear combinations of internal coordinates following the recommendations of Fogarasi et. al. [14] is summarized in Table 2. The theoretically calculated force fields were transformed into this set of vibrational coordinates and used in all subsequent calculations.

PREDICTION OF RAMAN INTENSITIES.

The Raman activities (Si) calculated with the GAUSSIAN 09W program were subsequently converted to relative Raman intensities (Ii) using the following relationship derived from the basic theory of Raman scattering [18]
Where ν0 is the exciting frequency in cm-1, νi the vibrational wavenumber of the ith normal mode, h, c, and k are the fundamental constants and f is a rightfully chosen ordinary normalization factor for all the peak intensities.

VI. RESULTS AND DISCUSSION

4.1 Molecular geometry

The optimized molecular structure of APH along with the numbering of atoms is shown in Fig. 1. The optimized structure parameters of APH obtained by DFT-B3LYP/ 6-311+G (d,p) and HF/ 6-311+G (d,p) levels are listed in Table 3. From the structural data given in Table 3, it is observed that the various bond lengths are found to be almost the same at HF/ 6-311+G(d,p) level of theory, in general slightly overestimates bond lengths but it yields bond angles in excellent agreement with the HF method.

The intended geometric parameters can be worn as a foundation to work out the other parameters for the compound. The optimized molecular configuration of APH reveals that the N- heterocyclic rings of the amino group are in planar. Inclusion of CH group and NH atoms known for its strong electron-withdrawing nature, in heterocyclic position, is expected to increase a contribution of the resonance structure, in which the electronic charge is concentrated at this site. This is the reason for the shortening of bond lengths N11-H12=0.994A0 and N11-H13=0.995A0 obtained by the HF method. The same bond lengths calculated by the DFT method is found to be 1.009A0 and 1.010A0. The carbon atoms are bonded to the hydrogen atoms with a σ-bond in the heterocyclic ring and the substitution of hydrogen atoms for hydrogen reduces the electron density at the ring carbon atom. In APH, the N-H bond lengths vary from 0.997A0 to 0.999 by the HF method and from 1.013 to 1.014 B3LYP methods. The ring carbon atoms in substituted heterocyclic exert a larger attraction on the valence electron cloud of the hydrogen atom resulting in an increase in the C-H force constants and a decrease in the corresponding bond length. It is evident from the C-C bond lengths ranging from 1.375A0 to 1.489 A0 by HF method and from 1.385 to 1.485 by B3LYP method in the heterocyclic rings of APH, whereas the C-H bond lengths in APH vary from 1.073A0 to1.076 A0 and

International Journal of Engineering Research & Technology (IJERT)
ISSN: 2278-0181
Vol. 9 Issue 01, January-2020

from 1.084 to 1.086A0 by HF and B3LYP methods, respectively. The heterocyclic rings appear to be a little distorted because of the NH2 group substitution as seen from the bond angles C3-C4-C5 which are calculated as 118.96º and 118.76º respectively, by HF and B3LYP methods and are smaller than the typical hexagonal angle of 120º. The comparative graphs of bond lengths, bond angles and dihedral angles of APH for three sets are presented in Figs. 2-4 respectively. From the theoretical values, it is found that most of the optimized bond lengths are slightly larger than the experimental values, due to that the theoretical calculations belong to isolated molecules in the solid phase and the experimental results belong to molecules in solid-state. Comparing bond angles and lengths of B3LYP with those of HF, as a whole the formers are bigger than later and the B3LYP calculated values correlate well compared with the experimental data.

4.2. First hyperpolarizability

The potential application of the title compound in the field of nonlinear optics demands, the investigation of its structural and bonding features contribution to the hyperpolarizability enhancement, by analyzing the vibrational modes using IR and Raman spectroscopy. Many organic molecules, containing conjugated π electrons are characterized by large values of molecular first hyperpolarizabilities, which were analyses through vibration spectroscopy [19]. In most of the cases, even in the absence of inversion symmetry, the strongest band in the IR spectrum is weak in the Raman spectrum and vice-versa. But the intramolecular charge from the donor to acceptor group through a π-bond conjugated path can induce large variations of both the molecular dipole moment and the molecular polarizability, manufacture of IR and Raman activity strong at the similar time. The experimental spectroscopic behavior described above is well accounted for calculations in π conjugated systems that predict exceptionally infrared intensities for the same normal modes. The primary hyperpolarizability (β) of this novel molecular system is calculated using the ab initio quantum mechanical method, based on the finite-field approach. In the presence of an applied electric field, the energy of a system is a function of the electric field. The primary hyperpolarizability is a third-rank tensor that can be described by a 3x3x3 matrix. The 27 mechanism of the 3D matrix can be synopsis to 10 mechanisms due to the Kleinman symmetry [20]. The mechanism of β is exact as the coefficients in the Taylor series swelling of the energy in the external electric field. When the electrical field is feeble and all the same, this growth becomes Where E0 is the energy of the unperturbed molecule; Fi is the field at the origin; and μi, αij βijk, and γijkl and are the components of dipole moment, polarizability, the first hyperpolarizabilities, and second hyperpolarizibilities, respectively. The calculated total dipole moment (μ) and mean first hyperpolarizability (β) of APH are 1.1437 Debye and 8.3541x10-30 esu, respectively, which is comparable with the reported values of similar derivatives. The large value of hyperpolarizibilities, β which is a measure of the non-linear optical activity of the molecular system, is associated with the intermolecular charge transfer, resulting from the electron cloud movement through π conjugated framework from an electron donor to electron acceptor groups. The physical properties of these conjugated molecules are governed by the high degree of electronic charge delocalization along the charge transfer axis and by the low band gaps. So we conclude that the title compound is an attractive object for future studies of nonlinear optical properties.

4.3. NMR spectral analysis

The isotropic chemical shifts are frequently used as an aid in the identification of reactive organic as well as ionic species. It is documented that correct predictions of molecular geometries are necessary for reliable calculations of magnetic properties. Therefore, the full geometry optimization of APH was performed by using the B3LYP/6-311+G (d,p) method. Then, Gauge-Including Atomic Orbital (GIAO) 1H and 13C chemical shift calculations of the compound have been made by the same method. Application of the GIAO [21] approach to molecular systems was significantly improved by an efficient application of the method to the ab initio SCF calculations, using techniques borrowed from analytic derivative methodologies. GIAO procedure is somewhat superior since it exhibits a faster convergence of the calculated properties upon extension of the basis set used. Taking into account the computational cost and the effectiveness of calculation, the GIAO method seems to be preferable from many aspects at the present state of this subject.

On the other hand, the density functional methodologies offer an effective alternative to the conventional correlated methods, due to their significantly lower computational cost. The molecular structure of APH is optimized by the B3LYP method with 6-311+G (d,p). Then, gauge-including atomic orbital (GIAO) 13C and 1H chemical shift calculation of title compound is made by using the B3LYP method. The 1H and 13C chemical shifts were measured in a less polar (CDCl3) solvent. The result in Table 4 shows that the range 13C NMR chemical shift of the typical organic molecule usually is >100 ppm [22,23], the accuracy ensures reliable interpretation of spectroscopic parameters.

It is true from the above literature value, in our present study, the title molecule APH also falls with the above literature data except with the carbon atoms (C4). In the present paper, the signal observed at 190.30 ppm in the 13C NMR spectrum is assigned to C10 carbon atom correlates with theoretically predicted value at 187.473 ppm. The signals for aromatic carbons were observed at 127.70 – 184.70 ppm in the 13C NMR spectrum for the title molecule, since those carbon atoms which belong to APH also exactly correlate with theoretically predicted value at 114.474 – 186.714 ppm. The signals of the aromatic proton were observed at 21.90 –22.03 ppm. The calculated (24.950-25.037 ppm) proton NMR chemical shifts show moderate agreement with the experimental

International Journal of Engineering Research & Technology (IJERT)
ISSN: 2278-0181
Vol. 9 Issue 01, January-2020

values except with aliphatic proton H16, H17. The H atom is the smallest of all atoms and mostly localized on the periphery of molecules. Therefore their chemical shifts would be more susceptible to intermolecular interactions in the aqueous solution as compared to that for other heavier atoms. Another important aspect is that hydrogen attached or nearby electron-withdrawing atom or group can decrease the shielding and moves the resonance of the attached proton towards a higher frequency. By contrast, electron-donating atom or group increases the shielding and moves the resonance on the way to a lower frequency. In this study, the chemical shifts obtained and calculated for the hydrogen atoms of amino groups are high. All values are [24] due to the shielding effect. It is true from above literature data in our present study the amino protons at N11 appears as singlet with two protons integral at 27.40 - 27.41 ppm shows good agreement with computed chemical shift (30.606-30.418) values are shown in Table 4. The relationship between the experimental chemical shift and computed GIAO/ B3LYP/ 6-311+G(d,p) levels for 13C and1H are shown in Fig 5.

4.4. HOMO-LUMO analysis

Many organic molecules that contain conjugated π electrons are characterized by hyperpolarizabilities and were analyzed using vibrational spectroscopy [23]. In most cases, even in the absence of inversion symmetry, the weakest bands in the Raman spectrum are strongest in the IR spectrum and vice versa. But the intramolecular charge transfer from the donor to the acceptor group through a single–double bond conjugated path can induce large variations of both the molecular dipole moment and the molecular polarizability, making IR and Raman activity strong at the similar time. It is also experimental in the title compound the bands in the FT-IR spectrum have their counterpart in Raman show that the relative intensities in IR and Raman spectra are similar resulting from the electron cloud movement through π conjugated casing work from an electron donor to electron acceptor groups. The highest engaged molecular orbital (HOMO) and lowest unlived in molecular orbital (LUMO) are very important parameters for quantum chemistry. We can conclude the way the molecule interacts with previous species; hence, they are called the frontier orbitals. HOMO, which can be thought the outermost orbital containing electrons, tends to give these electrons such as an electron donor. On the other hand; LUMO can be thought the innermost orbital containing free places to accept electrons [25]. outstanding to the interaction between HOMO and LUMO orbital of a structure, conversion state transition of π* type is observed about the molecular orbital theory. The calculated self-consistent field (SCF) energy of APH is -623.9 537 a.u. Therefore, while the energy of the HOMO is in a straight line related to the ionization potential, LUMO energy is directly linked to the electron affinity.

The energy difference between HOMO and LUMO orbitals is called an energy gap that is important stability for structures. Also, the pictorial scheme of a few MOs of APH is shown in Fig. 6. HOMO is localized on the central ring and has partially contribution from the substitution groups such as oxygen and amino group. LUMO is quite localized on the central ring and has a strong contribution from the substituted electronegative oxygen and amino group. The energy gap between HOMO and LUMO is 0.1058 a.u., which shows that charge transfer may be taking place from the ring to oxygen atom. As seen in Fig. 6, HOMO-1 is very similar to HOMO, rotated by 90◦. HOMO-3 is mainly localized on ring carbon atom whereas LUMO+3 is localized on ring carbon atoms and an oxygen atom. Homo -Lumo energy gap and related molecular properties of 4-aminophthalhydrazide from table 5

V.CONCLUSION

In this present investigation molecular structure, vibrational frequencies, HOMO, LUMO, and polarizability analysis of APH have been studied using ab initio HF and DFT (B3LYP/6-311+G(d,p)) calculation. The NMR (1H and 13C) spectral studies were carried out for the first time. Any discrepancy noted between the observed and calculated frequencies maybe because the calculations have been done on a single molecule in the solid-state contrary to the experimental values recorded in the presence of intermolecular interactions. Based on the agreement between the calculated and observed results, assignments of fundamental vibrational modes of APH were examined and some assignments are proposed. This study demonstrates that scaled DFT/B3LYP calculations are a powerful approach for understanding the vibrational spectra of the medium-sized organic compound. Temperature dependence of the thermodynamic properties heat capacity at constant pressure (Cp), entropy (S) and enthalpy change (ΔH0→T) for APH were also determined by B3LYP/6–311+G(d,p) method. The UV spectrum was calculated in an ethanol solution. The theoretically constructed FT-IR and FT-Raman spectrum shows a good correlation with experimentally observed FT-IR and FT-Raman spectrum.

International Journal of Engineering Research & Technology (IJERT)
ISSN: 2278-0181
Vol. 9 Issue 01, January-2020

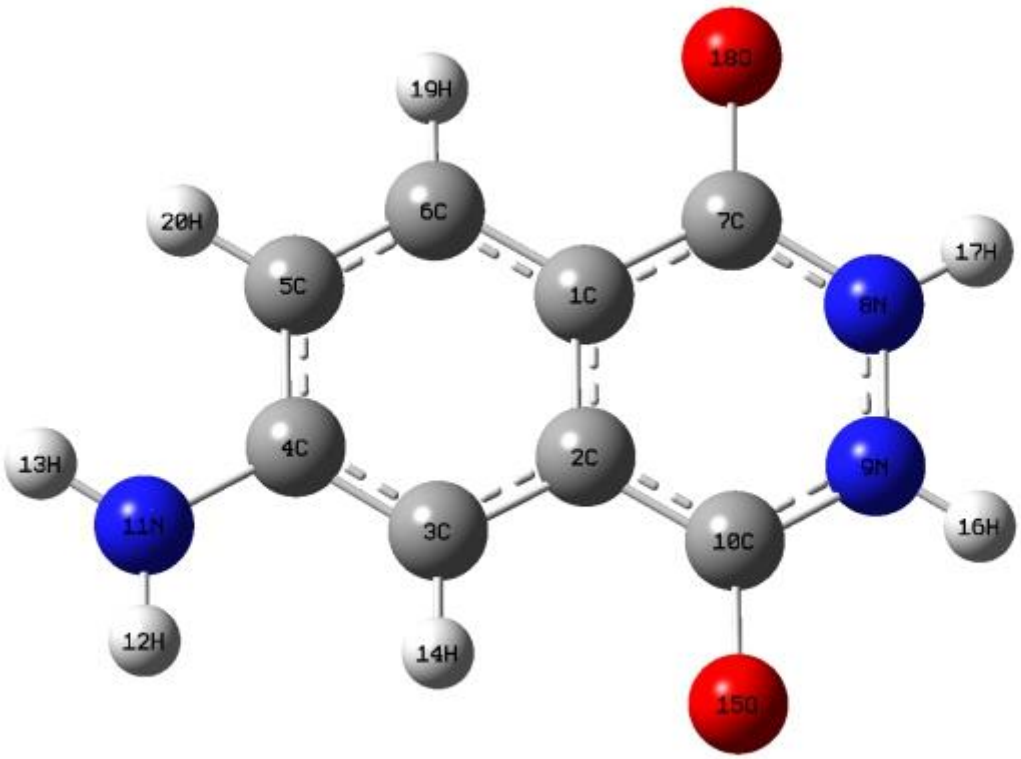

MOLECULAR STRUCTURE OF APH FIG.1

THE COMPARATIVE GRAPHS OF BOND LENGTHS, BOND ANGLES AND DIHEDRAL ANGLES OF APH FIG2-4

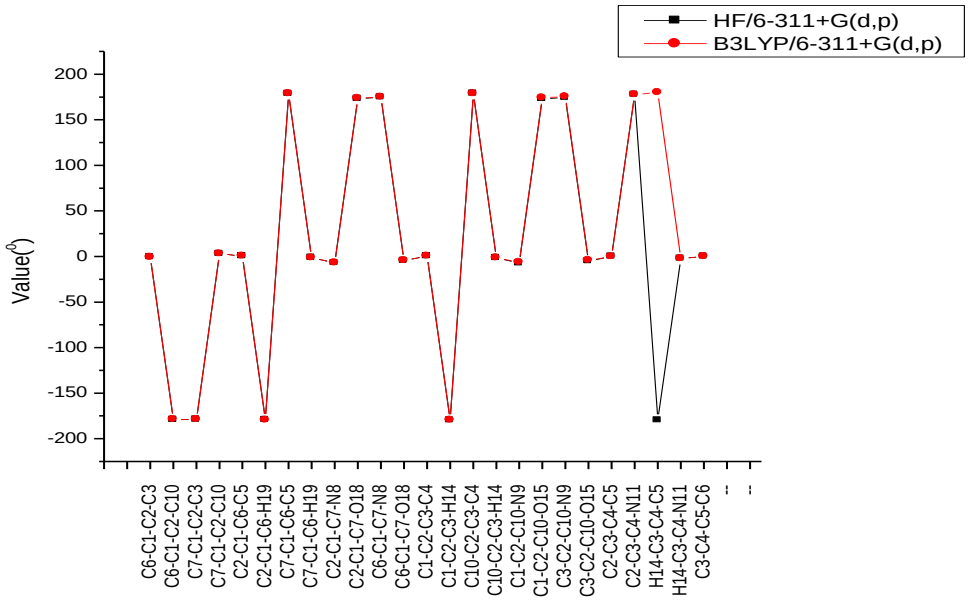

FIG2

International Journal of Engineering Research & Technology (IJERT)
ISSN: 2278-0181
Vol. 9 Issue 01, January-2020

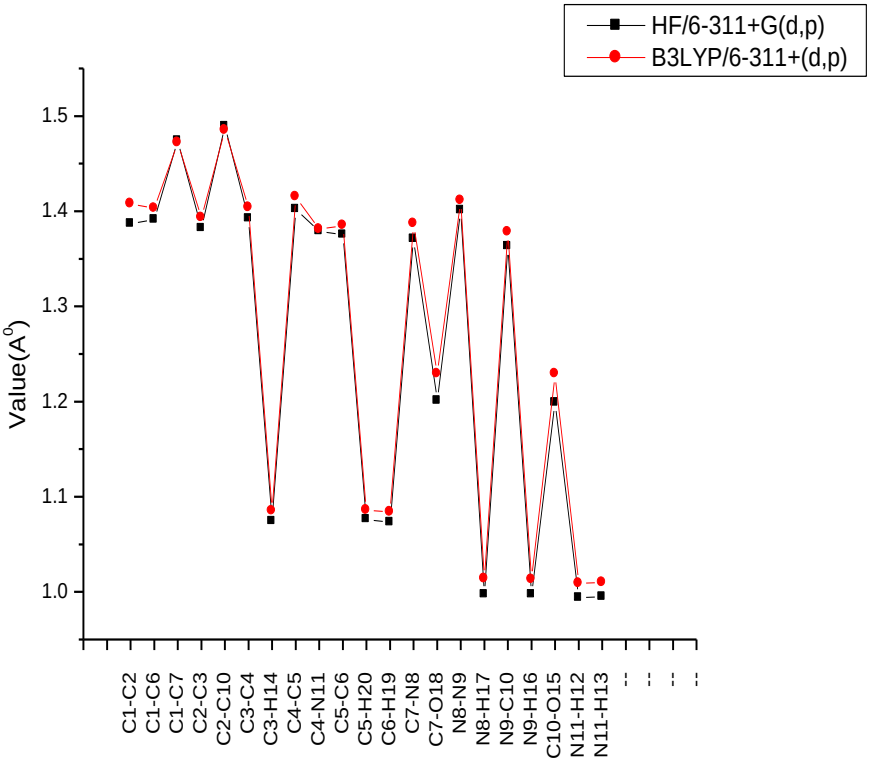

FIG3

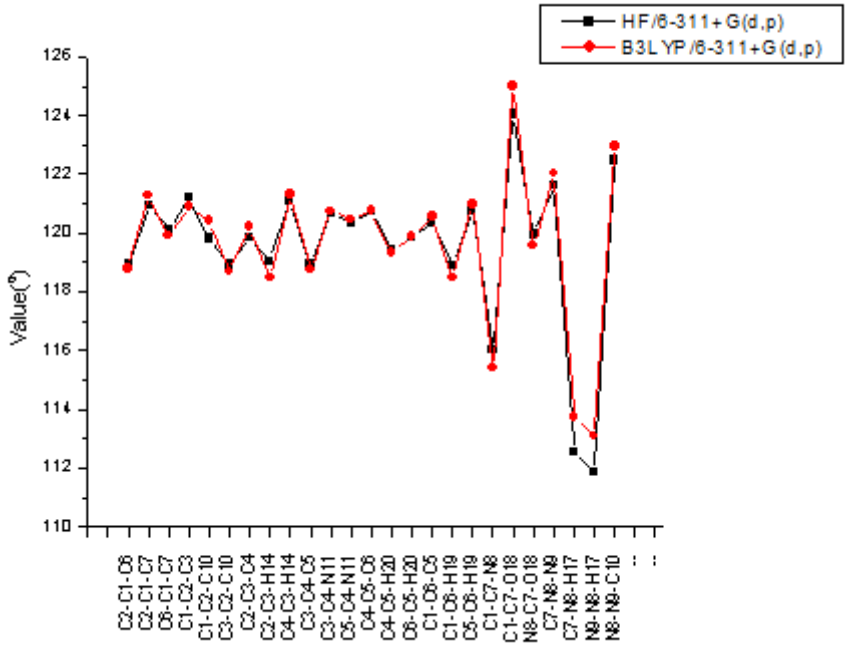

FIG4

International Journal of Engineering Research & Technology (IJERT)
ISSN: 2278-0181
Vol. 9 Issue 01, January-2020

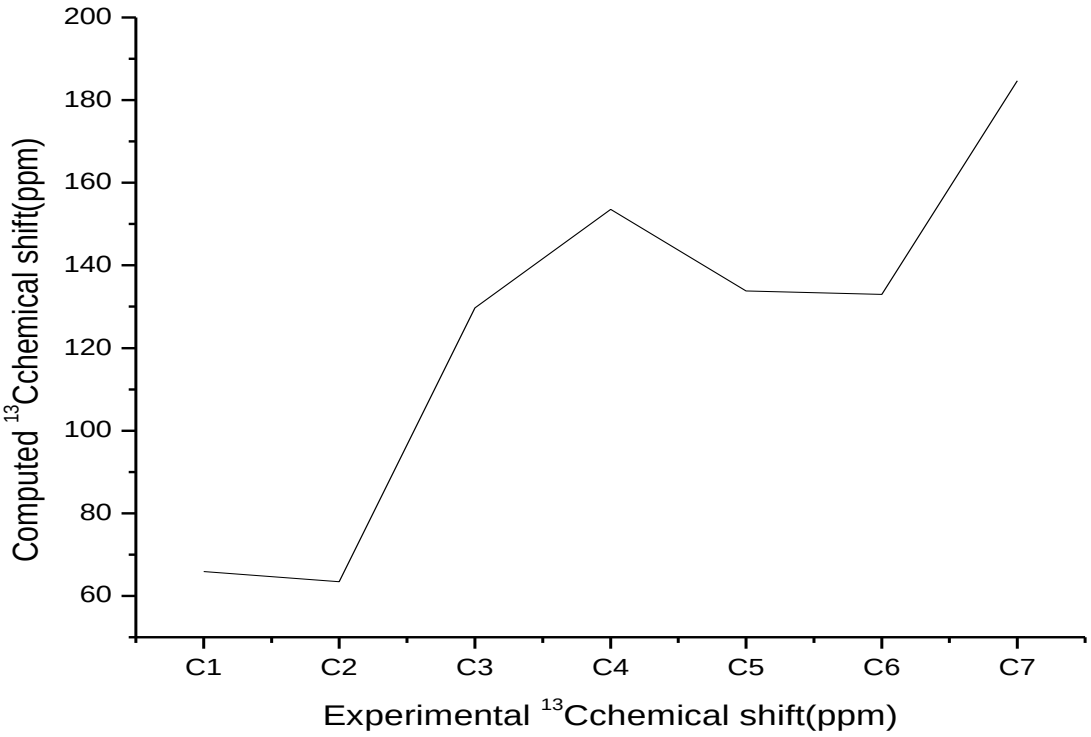

The relationship between the experimental chemical shift and computed GIAO/ B3LYP/ 6-311+G(d,p) levels for 13C and1H are shown in Fig 5.

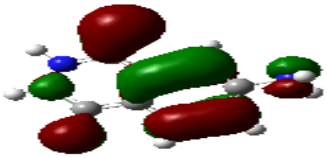

Homo-4 energy=-0.3389 a.u

Lumo+4 energy= -0.0382 a.u.

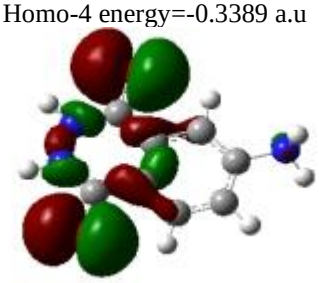

Homo-3 energy=-0.3359 a.u.

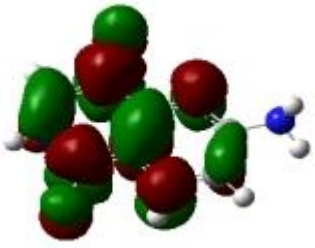

Lumo+3 energy= -0.0670 a.u.

International Journal of Engineering Research & Technology (IJERT)
ISSN: 2278-0181
Vol. 9 Issue 01, January-2020

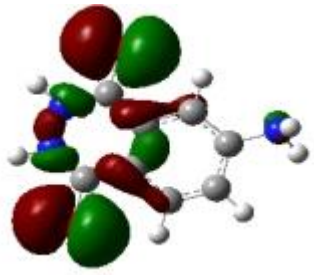

Homo-2 energy= -0.3351a.u.

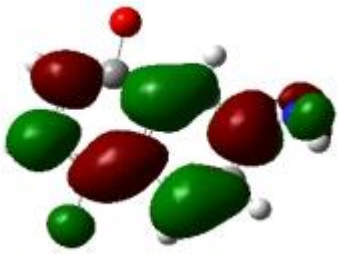

Lumo+2 energy= -0.0887 a.u.

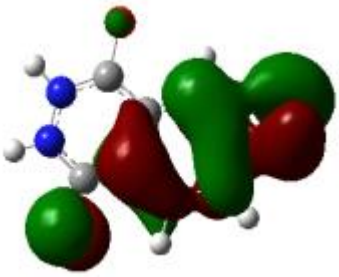

Homo-1 energy=-0.3243 a.u.

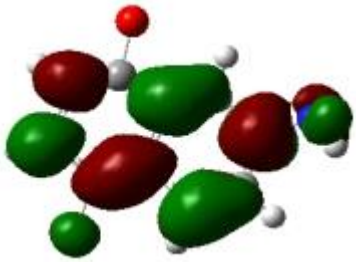

Lumo+1=-0.1707 a.u.

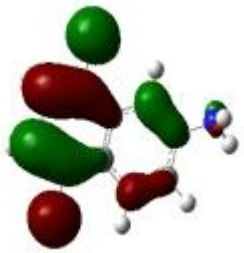

Homo energy=-0.2839a.u.

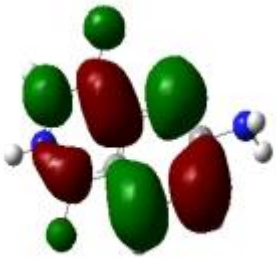

Lumo energy= -0.1781a.u.

Fig 6 energy gap between Homo- Lumo analysis.

Table 1
Definition of internal coordinates of 4-aminophthalhydrazide

No. (i)	Symbol	Type	Definition[a]
Stretching			
1-3	R_i	C-H	C_3 - H_{14}, C_5- H_{20},C_6- H_{19}
4-11	r_i	C-C	C_1-C_2, C_2-C_3, C_3-C_4,C_4-C_5, C_5-C_6, C_6-C_1,C_1-C_7, C_2-C_{10}
12	S_i	N-N	N_8- N_9
13-15	q_i	N-C	N_8-C_7, N_9-C_{10} ,N_{11}-C_4
16-17	P_i	N-H	N_8-H_{16}, N_9-H_{17}
18,19	x_i	C-O	C_7-O_{18}, C_{10}-O_{15}
20,21	Q_i	NH_2	N_{11}-H_{12}, N_{12}-H_{13}
In-plane bending			
22-27	α_i	Ring1	C_1-C_2-C_3, C_2-C_3-C_4, C_3-C_4-C_5, C_4-C_5-C_6, C_5-C_6- C_1, C_6-C_1-C_2
28-33	α_i	Ring2	C_7-N_8-N_9, N_8-N_9-C_{10}, N_9-C_{10}-C_2, C_{10}-C_2-C_1, C_2-C_1-C_7, C_1-C_7-N_8
34-39	β_i	C-C-H	C_1-C_6-H_{19},C_5-C_6-H_{19},C_6-C_5-H_{20},C_4-C_5-H_{20},C_2-C_3-H_{14},C_4-C_3-H_{11}
40,41	b_i	C-N-H	C_7-N_8-H_{17}, C_{10}-N_9-H_{16}
42,43	g_i	N-N-H	N_9-N_8-H_{17}, N_8-N_9-H_{16}
44,45	Z_i	C-C-O	C_1-C_7-O_{18},C_2-C_{10}-O_{15}
46,47	L_i	N-C-O	N_8-C_7-O_{18},N_9-C_{10}-O_{15}
48,49	X_i	C-C-N	C_3-C_4-N_{11}, C_5-C_4-N_{11}
50-51	M_i	C-N-H	C_4-N_{11}-H_{12}, C_4-N_{11}-H_{12}
52	T_i	H-N-H	H_{12}-N_{11}-H_{13}
53,54	d_i	N-N-H	N_9-N_8-H_{17}, N_8-N_9-H_{16}

International Journal of Engineering Research & Technology (IJERT)
ISSN: 2278-0181
Vol. 9 Issue 01, January-2020

Out-of-plane bending			
55-57	ψ_i	C-H	H_{14}-C_3-C_2-C_4, H_{19}-C_6-C_5-C_1, H_{20}-C_5-C_6-C_4
58-60	ρ_i	H-N	H_{16}-N_9-C_{10}-N_8, H_{17}-N_8- N_9-C_7, C_4-N_{11}-H_{12}-H_{13}
61-62	χ_i	C-O	O_{15}-C_{10}-N_9-C_2, O_{18}-C_7-N_8-C_1
Torsion			
63–68	τ_i	t Ring	C_1 - C_2 - C_3 - C_4, C_2 - C_3 - C_4 - C_5, C_3 - C_4 – C_5 - C_6, C_4 - C_5 - C_6 - C_1, C_5 - C_6 -C_1 - C_2, C_6 - C_1 - C_2 - C_3
69–74	τ_i	t Ring	C_7 - C_8 - C_9 - C_{10}, C_8 - C_9 - C_{10} - C_2, C_9 - C_{10} - C_2 - C_1,C_{10} - C_2 - C_1 - C_7, C_2 - C_1 - C_7 - C_8, C_1 - C_7 - C_8 - C_9
75	τ_i	t C-NH_2	C_4-N_{11}-H_{12}-H_{13}
76,77	τ_i	Butterfly	C_6- C_1 - C_2-C_{10}, C_7- C_1 - C_2-C_3

[a]For numbering of atoms refer FigTable 2

Table 2
Definition of local symmetry coordinates of 4-aminophthalhydrazide

No. (i)	Type	Definition[a]
1-3	C H	R_1,R_2,R_3
4-11	CC	r_4 ,r_5 ,r_6, r_7 ,r_8 ,r_9 ,r_{10} ,r_{11}
12	NN	S_{12}
13-15	NC	q_{13}, q_{14},q_{15}
16,17	NH	p_{16}, p_{17}
18,19	CO	X_{18}, x_{19}
20	NH_2ss	$(Q_{20}+Q_{21}) / \sqrt{2}$
21	NH_2ips	$(Q_{20}-Q_{21}) / \sqrt{2}$
22	R_1trigd	$(\alpha_{22} - \alpha_{23} + \alpha_{24} - \alpha_{25} + \alpha_{26} - \alpha_{27}) / \sqrt{6}$
23	R_1symd	$(-\alpha_{22} - \alpha_{23} + 2\alpha_{24} - \alpha_{25} - \alpha_{26} - 2\alpha_{27}) / \sqrt{12}$
24	R_1asymd	$(\alpha_{22} - \alpha_{23} + \alpha_{25} - \alpha_{26}) / \sqrt{2}$
25	R_2trigd	$(\alpha_{28} - \alpha_{29} + \alpha_{30} - \alpha_{31} + \alpha_{32} - \alpha_{33}) / \sqrt{6}$
26	R_2symd	$(-\alpha_{28} - \alpha_{29} + 2\alpha_{30} - \alpha_{31} - \alpha_{32} - 2\alpha_{33}) / \sqrt{12}$
27	R_2asymd	$(\alpha_{28} - \alpha_{29} + \alpha_{31} - \alpha_{32}) / \sqrt{2}$
28-30	b C H	$(\beta_{34} - \beta_{35}) / \sqrt{2}$, $(\beta_{36} - \beta_{37}) / \sqrt{2}$,$(\beta_{38}-\beta_{39}) / \sqrt{2}$
31	b NH	b_{40}- b_{41} / $\sqrt{2}$,g_{42} -g_{43}/ $\sqrt{2}$
32	b NN	g_{42} -g_{43}/ $\sqrt{2}$
33,34	b CO	$(Z_{44}-Z_{45}) / \sqrt{2}$, $(L_{46}-L_{47})/ \sqrt{2}$
35,36	b CN	X_{48}-X_{49}/ $\sqrt{2}$,M_{50}-M_{51}/ $\sqrt{2}$
37,38	b NH	T_{52} , $(d_{53} - d_{54}) / \sqrt{2}$
39-41	ω C H	ψ_{55} ,ψ_{56},ψ_{57}
42-44	ω NH	ρ_{58}, ρ_{59}, ρ_{60}
45,46	ω CO	χ_{61} ,χ_{62}
47	Ring trigd	$(\tau_{63} - \tau_{64} + \tau_{65} - \tau_{66} + \tau_{67} - \tau_{68}) / \sqrt{6}$
48	Ring symd	$(\tau_{63} - \tau_{65} + \tau_{66} - \tau_{68}) / \sqrt{2}$
49	Ring asymd	$(-\tau_{63} + 2\tau_{64} - \tau_{65} - \tau_{66} + 2\tau_{67} - \tau_{68}) / \sqrt{12}$
50	Ring trigd	$(\tau_{69} - \tau_{70} + \tau_{71} - \tau_{72} + \tau_{73} - \tau_{74}) / \sqrt{6}$
51	Ring symd	$(\tau_{69} - \tau_{71} + \tau_{72} - \tau_{73}) / \sqrt{2}$
52	Ring asymd	$(-\tau_{69} + 2\tau_{70} - \tau_{71} - \tau_{72} + 2\tau_{73} - \tau_{74}) / \sqrt{12}$
53	t C-NH_2	τ_{75}
54	Butterfly	$(\tau_{76} - \tau_{77}) / \sqrt{2}$

[a]The internal coordinates used here are defined in Table 1.

International Journal of Engineering Research & Technology (IJERT)
ISSN: 2278-0181
Vol. 9 Issue 01, January-2020

Table 3
Optimized geometrical parameters of 4-aminophthalhydrazide obtained by HF/6-311+G (d,p) and B3LYP /6-311G+(d, p) density functional theory calculations

Bond length	Value (Å)		Exp[a]	Bond angle	Value (°)		Exp[a]
	HF/6-311+G(d,p)	B3LYP/6-311+G(d,p)			HF/6-311+G(d,p)	B3LYP/6-311+G(d,p)	
C1-C2	1.387	1.408	1.359	C2-C1-C6	118.96	118.78	120.3
C1-C6	1.391	1.403	1.383	C2-C1-C7	120.94	121.27	121.7
C1-C7	1.474	1.472		C6-C1-C7	120.12	119.91	119.8
C2-C3	1.382	1.393	1.415	C1-C2-C3	121.22	120.88	121.6
C2-C10	1.489	1.485		C1-C2-C10	119.81	120.41	
C3-C4	1.392	1.404	1.423	C3-C2-C10	118.93	118.67	
C3-H14	1.074	1.085	0.917	C2-C3-C4	119.82	120.21	116.4
C4-C5	1.402	1.415	1.391	C2-C3-H14	119.05	118.47	
C4-N11	1.379	1.381	1.347	C4-C3-H14	121.11	121.30	
C5-C6	1.375	1.385	1.364	C3-C4-C5	118.96	118.76	121.1
C5-H20	1.076	1.086	0.884	C3-C4-N11	120.66	120.74	122.5
C6-H19	1.073	1.084	0.920	C5-C4-N11	120.33	120.45	119.8
C7-N8	1.371	1.387		C4-C5-C6	120.72	120.77	119.6
C7-O18	1.201	1.229		C4-C5-H20	119.41	119.34	121.7
N8-N9	1.401	1.411		C6-C5-H20	119.85	119.88	
N8-H17	0.997	1.014	0.872	C1-C6-C5	120.34	120.56	
N9-C10	1.363	1.378	1.460	C1-C6-H19	118.92	118.47	120.3
N9-H16	0.999	1.013	1.405	C5-C6-H19	120.73	120.96	123.3
C10-O15	1.199	1.229		C1-C7-N8	116.00	115.41	
N11-H12	0.994	1.009	0.908	C1-C7-O18	124.04	125.00	
N11-H13	0.995	1.010	0.887	N8-C7-O18	119.95	119.57	
				C7-N8-N9	121.61	122.02	119.8
				C7-N8-H17	112.55	113.73	115.2
				N9-N8-H17	111.85	113.08	
				N8-N9-C10	122.47	122.95	

International Journal of Engineering Research & Technology (IJERT)
ISSN: 2278-0181
Vol. 9 Issue 01, January-2020

TABLE-4
3LYP /6-311G+(d, p) density functional theory calculations

Bond length	Value (Å)			Bond angle	Value (°)		
	HF/6-311+G(d,p)	B3LYP/6-311+G(d,p)	Exp[a]		HF/6-311+G(d,p)	B3LYP/6-311+G(d,p)	Exp[a]
C1-C2	1.387	1.408	1.359	C2-C1-C6	118.96	118.78	120.3
C1-C6	1.391	1.403	1.383	C2-C1-C7	120.94	121.27	121.7
C1-C7	1.474	1.472		C6-C1-C7	120.12	119.91	119.8
C2-C3	1.382	1.393	1.415	C1-C2-C3	121.22	120.88	121.6
C2-C10	1.489	1.485		C1-C2-C10	119.81	120.41	
C3-C4	1.392	1.404	1.423	C3-C2-C10	118.93	118.67	
C3-H14	1.074	1.085	0.917	C2-C3-C4	119.82	120.21	116.4
C4-C5	1.402	1.415	1.391	C2-C3-H14	119.05	118.47	
C4-N11	1.379	1.381	1.347	C4-C3-H14	121.11	121.30	
C5-C6	1.375	1.385	1.364	C3-C4-C5	118.96	118.76	121.1
C5-H20	1.076	1.086	0.884	C3-C4-N11	120.66	120.74	122.5
C6-H19	1.073	1.084	0.920	C5-C4-N11	120.33	120.45	119.8
C7-N8	1.371	1.387		C4-C5-C6	120.72	120.77	119.6
C7-O18	1.201	1.229		C4-C5-H20	119.41	119.34	121.7
N8-N9	1.401	1.411		C6-C5-H20	119.85	119.88	
N8-H17	0.997	1.014	0.872	C1-C6-C5	120.34	120.56	
N9-C10	1.363	1.378	1.460	C1-C6-H19	118.92	118.47	120.3
N9-H16	0.999	1.013	1.405	C5-C6-H19	120.73	120.96	123.3
C10-O15	1.199	1.229		C1-C7-N8	116.00	115.41	
N11-H12	0.994	1.009	0.908	C1-C7-O18	124.04	125.00	
N11-H13	0.995	1.010	0.887	N8-C7-O18	119.95	119.57	
				C7-N8-N9	121.61	122.02	119.8
				C7-N8-H17	112.55	113.73	115.2
				N9-N8-H17	111.85	113.08	
				N8-N9-C10	122.47	122.95	

Table 5
HOMO - LUMO energy gap and related molecular properties of 4-aminophthalhydrazide

Molecular Properties	B3LYP/6-311+G(d,p)
HOMO	-0.2839a.u
LUMO	-0.1781a.u.
Energy gap	0.1058 a.u.
Ionisation Potential (I)	0.2839 a.u.
Electron affinity(A)	0.1781a.u.
Global softness(s)	18.9035 a.u.
Global Hardness (η)	0.0529 a.u.
Chemical potential (μ)	-0.231 a.u.
Global Electrophilicity (ω)	0.5043 a.u.

International Journal of Engineering Research & Technology (IJERT)
ISSN: 2278-0181
Vol. 9 Issue 01, January-2020

REFERENCES

[1] K.S. Markley, Fatty Acids, Their Chemistry Properties and Uses, Interscience Publishers, New York, 1964, pp.1604-1608.
[2] E.A. Yousef, M.E.Zaki, M.G.Megahed, Heterocyclic. Commun. 9 (2003) 293-298.
[3] D.L. Trepanier, E.R.Wagner, G.Harris, A.D.Rudzik, J.Med. Chem. 9 (1996) 881-885.
[4] K.K.Bedia, O.Elcin, U.Seda, K.Fatma, S.Nathaly, R.Sevim, A.Dimoglo, Eur .J. Med. Chem. 41 (2006) 1253-1261.
[5] H.Yin, J. Cui, Y. Qiao, Polyhedron 27 (2008) 2157-2166.
[6] G.M.Sheldrick, Acta Cryst. A64 (2008) 112-122.
[7] V.Arjunan, T.Rani, C.VMythili, S.Mohan Spectrochim. Acta A79 (2012) 486-496.
[8] J.R.Durig, S.F.Bush, E.E.Mercer, J.Chem.Phys.44 (1967) 4238.
[9] V. Krishnakumar,K.Parusuraman, A.Natarajan, *Ind.J.Pure Appl. Phys.* 56 (1998) 171.
[10] Gaussian 09 Program, Gaussian Inc., Wallingford CT., 2009.
[11] A.D.Becke,J.Chem. Phys. 98(1993)5648-5652.
[12] C.Lee, W.Yang, R.G.Parr. Phys. Rev. B37 (1988) 785-789.
[13] P.Pulay, G. Fogarasi, G.Pongor, J.E.Boggs, A.Vargha, J. Am. chem. soc,105 (1983) 7037- 047.
[14] G. Fogarasi, P.Pulay,in: J.R.Durig(Ed.) Vibrational Spectra and Structure, Vol.14, Elsevier, Amsterdam, 1985 , P. 125, Chapter 3.
[15] T.Sundius, vib, spectrosc.29 (2002)89-95.
[16] MOLVIB (V.7.0):Calculation of Harmonic Force Fields and Vibrational Modes of Molecules, QCPE Program No. 807(2002).
[17] L. Wen, H. Yin, W. Li, K. Li, Acta Cryst. E 65 (2009) o2623.
[18] P.L. Polavarapu, J. Phys. Chem. 94 (1990) 8106-8112.
[19] J.Karpagam, N.Sundaraganesan, S.Sebastain, S.Manoharan, M.Kurt, J. Raman Spectrosc, 41 (2010) 53-62.
[20] D.A.Kleinman, Phys. Rev.126 (1962) 1977-1979.
[21] R. Ditchfield, Mol. Orbit. Theory Magn. Shielding Magn. Susceptibility 56 (1972) 5688.
[22] Y. Ataly, D. Avai, A. Basoglu, Struct. Chem. 19 (2008) 239.
[23] T. Vijayakumar, I. Hubert Joe, C.P.R. Nair, V.S. Jayakumar, Chem. Phys. 343 (2008)
[24] M. Karabacak, M. Cinar, M. Kurt, J. Mol. Struct. 968 (2010) 108.
[25] M. Arivazhagana,R.Meenakshi Spectrochim. Acta A91 (2012) 419-430.